

Velocity and texture of a plasma jet created in a plasma torch with fixed minimal arc length

M Vilotijevic¹, B Dacic² and D Bozic³

¹ Plasma Jet Co, Branicevska 29, 11000 Beograd, Serbia

² Plasma Jet Co, 8/14 Willcott St, 1025 Auckland, New Zealand

³ Inst. Nucl. Sci. 'Vinca', PO Box 522, Beograd, Serbia

E-mail: vilotijevic@plasmajet.info

Received 21 May 2008, in final form 29 October 2008

Published 16 January 2009

Online at stacks.iop.org/PSST/18/015016

Abstract

A new plasma jet (PJ-100) plasma spraying torch with a fixed minimal arc length was tested and the basic working parameters were measured and evaluated. The velocity of the plasma exiting both the cylindrical and the conical anode nozzles was assessed by measuring the thrust generated by the plasma jet and by photographing the translation of plasma clouds (parts with different brightnesses) in the last third of the length of the plasma plume. The basic characteristics of the argon/hydrogen plasma jets (enthalpy, mean temperature, mean plasma velocity and effective exhaust thrust velocity) were determined for different working regimes, for both the cylindrical and the conical nozzles. The thermal efficiency of the new plasma torch is between 70% and 74% for the plasma generation power up to 90 kW. The plasma plume generated in the cylindrical nozzle has a homogeneous radial temperature (and velocity) distribution with a full laminar flow.

1. Introduction

The quality of plasma sprayed coating depends directly on the heat and momentum transferred from the plasma to the particles injected into the plasma plume. For a chosen plasma gas composition the heat and momentum transfer vary with: (i) the velocity and temperature of the plasma, (ii) the radial temperature and velocity distribution in the plasma plume, (iii) the length of the plasma plume and (iv) the dwelling time of particles in the plasma. All these parameters of the generated plasma depend on the working power of the plasma torch and its construction.

Most operational plasma torches today have a conventional construction consisting of a cone shaped cathode and a hollow anode [1]. This design possesses a well-known limitation, namely, a short arc path with both high azimuthal and axial oscillations [2]. As a result, the conventional design of the plasma gun has an unfavourable voltage–current regime (it operates in a low voltage and high current mode), a low coefficient of thermal efficiency of 40–50% and a non-uniform hitting of the plasma gas, producing therefore a plasma jet of

very turbulent nature with a large axial and a radial temperature oscillation [3].

In many respects the existing conventional plasma spraying torches have reached their technical and technological limits for further quality and cost advancement in plasma coating and plasma forming of near-to-net shape parts. In the last few decades a couple of new plasma torch designs have emerged, each aiming to extend the length of the arc and hence to generate a plasma jet with a higher temperature homogeneity and a better voltage–current working regime. Metco Co achieved it with the so-called APG construction by mechanically separating the cathode from the anode upon ignition of the plasma [4], and Osram Sylvania Inc. did so by inserting an 'inter-electrode' between the cathode and the anode [5]. In the latter construction, the diameter of the cylindrical anode nozzle was larger than the diameter of the cylindrical 'inter-electrode' opening, and additional gas was injected at the zone of contact of the two nozzles for fixation of the anodic arc root. The design with two anode nozzles, powered with independent currents controlling each of the anodes [6], is yet another interesting torch design. Different designs of a 'cascade arc', where an 'inter-electrode' was

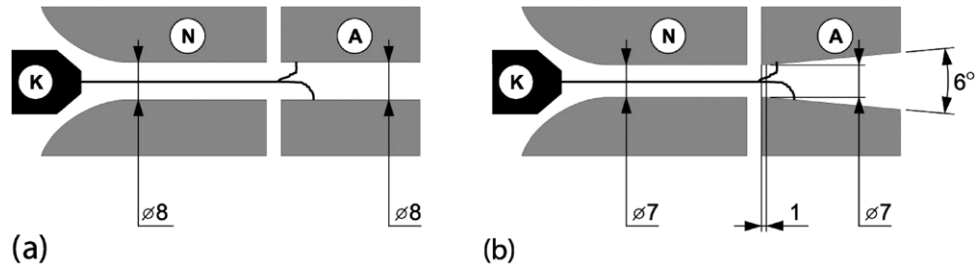


Figure 1. Schematic of the PJ-100 dc arc plasma torches: cylindrical nozzle (a) and conical nozzle (b).

replaced by ceramic and copper rings packed in succession, belong to yet another class of plasma gun design. An example is the TRIPLEX torch with three such cathodes instead of one, a construction which ‘splits’ the total current into three independent arc currents [1, 3].

The PJ-100 plasma torch [7] was developed to meet the need for a faster, lengthier and temperature homogeneous plasma jet. The PJ-100 plasma spraying torch with a maximum power of 100 kW was designed and manufactured by Plasma Jet Co.

This study evaluates the basic working characteristics measured for a new design plasma torch: the current–voltage characteristic, the thermal efficiency and the texture and velocity of the plasma jet. The plasma velocity was evaluated by two contactless methods. Measurement of thrust was one method, which is often applied for assessment of the plasma velocity and performances of plasma torches used as arc thrusters [8, 9]. Taking photographs of the plasma plume was the second method, which revealed important general dynamical characteristics of the plasma, enabling an assessment of plasma jet velocity. Recording changes in plasma velocity, noting both the texture of the plasma plume (axial and radial gradient of brightness) and the length of the plasma plume are functions of the basic working parameters of the plasma torch (power, gas flow rate and thermal losses). For the two different nozzle designs, conical and cylindrical, the two methods were applied for plasma velocity assessment, allowing optimization of the working parameters of the PJ-100 plasma torch.

2. Experimental methodology

The plasma torch in figure 1, evaluated in this study, possesses fixed minimal arc length, the fixation being achieved by an inserted cylindrical electrically neutral copper nozzle (N)—‘neutrode’—inserted between the cathode (K) and the anode (A). Gas is introduced in a vortex regime into the space between the cathode and the neutrode. The 2 mm thick ceramic insulating ring separates the neutrode from the anode nozzle. The distance between the cathode tip and the anode opening is 32 mm, and the length of the anode is 30 mm. The anode, neutrode and cathode are all water cooled. This paper presents results obtained for two different anode nozzle designs, a cylindrical nozzle with a diameter of 8 mm (figure 1(a)) and a conical nozzle, which begins with a diameter of $d = 7$ mm and which conically expands with a widening angle of 6° (7 mm/ 6°), figure 1(b).

The acquisition of the measured data in the voltage signals was done by an interfacing eight-channel system comprising four isolated channels, A/D card (ED300) and a Pentium 3 (566 MHz) PC. Each of the used channels was calibrated in accordance with the expected voltage signal recorded by a digital multi-meter with high accuracy.

The working current (I) in the powered plasma torch was determined by measuring the voltage drop in a high-precision resistor (60 mV/600 A). The voltage drop (U) in the torch was measured from voltage taps attached directly to the torch. The standard calorimetric method was used to measure the thermal efficiency of the plasma torch. Thermal efficiency was calculated from the following equation:

$$\eta = 1 - \frac{Q}{P}, \quad (1)$$

where P is the total power of the plasma gun ($P = UI$) and Q is the heat dissipated through the cooling water of the plasma gun. The thermal loss in the plasma torch was determined by measuring the flow rate of the cooling water and the temperature difference of the cooling water flowing in and out of the torch:

$$Q = G_w \times C \times \Delta T, \quad (2)$$

where G_w is the water flow rate, volumetrically determined at 1.175 ± 0.004 L s $^{-1}$ (standard deviation of all measurements), C is the specific heat of water (4.18 J g $^{-1}$ K $^{-1}$) and ΔT is the increase in the water temperature. The temperature of the cooling water was measured by two type-K thermocouples, in opposite connection, mounted at the water inlet and outlet. Since this method measures only the temperature difference of the coolant, any absolute error of the type-K thermocouple can be eliminated. The cold junctions of thermocouples were kept in an ice/water mixture to preclude cold junction response on any possible fluctuation of the surrounding temperature.

Enthalpy of the plasma gas (H) was calculated from the energy conservation equation (3) applied to plasma generation [10], by evaluation of the heat balance of the plasma torch using the calorimetric data:

$$GH_0 + P_{ef} = GH + \frac{1}{2}Gv^2, \quad (3)$$

$$\Delta H = (P_{ef} - Gv^2/2)/G, \quad (4)$$

where G is the mass gas flow rate (kg s $^{-1}$), H is the enthalpy of plasma gas, H_0 is the enthalpy of the inlet gases and v is

the plasma velocity, $P_{ef} = \eta P = \eta UI$ is the effective power absorbed by the plasma.

The total energy of the generated plasma is partitioned as the enthalpy of the plasma gas and the kinetic energy of the plasma— $1/2 Gv^2$, the element in equation (3). It is possible to calculate the mean plasma temperature by evaluating the enthalpy (ΔH) from equation (4), even neglecting its kinetic energy term, as reported elsewhere [10]. In our study, the correction of ΔH for the kinetic energy term was made by estimation of the plasma velocity based on the measured plasma thrust—‘effective exhaust thrust velocity’ (v_e). The mean plasma temperature calculation, based on the assessed values for mean bulk enthalpy, provides a good insight into the variation of the plasma temperature with the different plasma generation parameters. Assuming that the generated plasma is isothermal, this value of mean plasma temperature, in accordance with equation (5), was used to calculate the sound velocity of the plasma (a_0).

$$a_0 = \sqrt{\gamma RT}. \quad (5)$$

Values of sound velocities obtained in this way were used as ‘referential’ when we compared the velocities of the generated plasma jets obtained by the two methods described in the rest of this paper. The corrected R value for the mean molar mass of the plasma gas and the adiabatic coefficient γ value of 1.65 were adopted in the conducted calculation, because the dissociation of hydrogen was completed in the temperature range of 10.000 K and at a pressure of 0.1 MPa [11].

The photographs of the plasma plume were taken by an IMACON 790 electronic camera with a 1×10^6 plug-in module, which enables taking of 10^6 photographs per second, with an exposure time of 200 ns. For any new chosen geometry of shooting (the camera positioning to the plasma plume and zooming) a calibrating photograph was made. Six to eight successive shots, with $1 \mu s$ time lapse between the two consecutive shots, were taken. The photographs are small ($16 \times 18 \text{ mm}^2$), and their analysis is possible only after careful computer processing, a procedure which enabled us to choose the best contrast and appropriate enlargement ($4 \times$) for further analysis of the photographs. This method of photographing the plasma plume allowed for estimation of the plasma speed in parts of the plasma plume in which it was possible to discriminate from the brighter to the darker zones, i.e. zones of different temperatures.

With the real coordinate grid superimposed on the photographs of the plasma plumes it was possible to measure the movement of the plasma clouds and, using these data, the local velocity of the plasma jet ($v = \Delta X / \Delta t$) was calculated. Due to very good stability of the oscillator plugged in to the camera, any error of speed measurements was actually just the error of the recording of the plasma cloud movement. The absolute error of the speed measurement (of $\pm 110 \text{ m s}^{-1}$) corresponds to the resolution of the four-times-magnified photographs.

An example of the photographed movement of the plasma cloud is shown in figure 2. In two successive photos, the movement shows discernible bright zones in the last third of the plasma plume, as can be seen most clearly at the ‘crosshair’

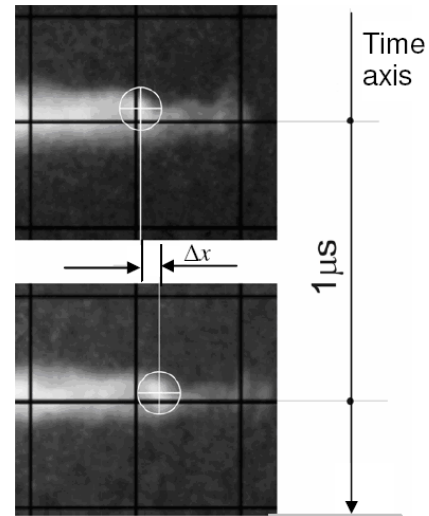


Figure 2. Two consecutive photographs of the part of the plasma plume in movement.

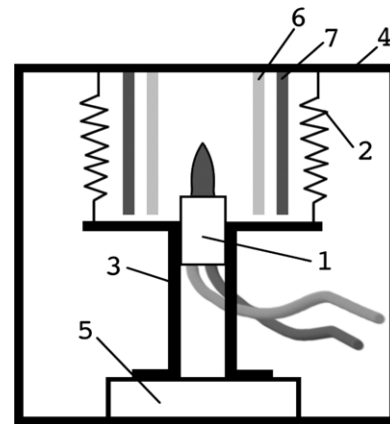


Figure 3. Experimental setup for plasma thrust measurement: plasma torch (1), the torch supporting carrier (3), measuring cell (5), coil suspensors (2), carrying frame–cage of the whole setup (4) and thermal shields (6 and 7).

position part at its centre. By following the movements of all the discriminated clouds it was possible to calculate the speed of each of these clouds. The average cloud speed with 30–40 measurements for each working regime was used for the estimation of the ‘mean plasma velocity’ (v).

The plasma spraying torch behaves like any other reactive engine and thus, for a given gas mass flow rate (G), the measured plasma thrust (F_t) from equation (6) can be used to calculate the effective exhaust velocity (v_e):

$$F_t = Gv_e. \quad (6)$$

The thrust of the plasma jet was experimentally measured by the thrust measurement setup presented in figure 3. The plasma torch was mounted with the nozzle in an upright position. The system of the coil suspensors balances the total weight of the plasma torch and the power supply leads to reducing the total load of the setup within the gauge range of the measuring head.

The head measures the force in the range 0–49 N with a sensitivity of 0.0098 N. Thermal shields 6 and 7, both

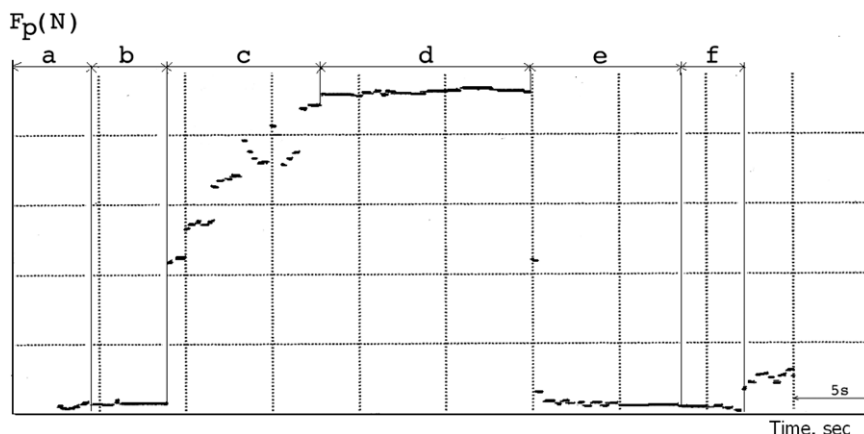


Figure 4. Typical recorded curve of the thrust force during the entire thrust measurement cycle.

10 mm thick, are made of pyrolytic carbon and asbestos plate, respectively. They protect the suspension coils from the heat emitted by the plasma plume, preserving the constant strength (elasticity) of balancing the suspensions during the entire measurement cycle. Simultaneously with the measurement of the plasma jet thrust, calorimetric measurement of the thermal efficiency of the plasma torch was conducted. After each cycle of plasma thrust measurement, the calibration of the measuring system was carried out by a ‘deadweight’ technique, where the plasma torch was additionally loaded with a known weight.

A typical measure thrust force cycle is recorded in figure 4. The range a relates to the stage when both the open-circuit voltage and the circulation of the cooling water were ‘on’. The range b in the diagram is connected with a detected small thrust provided by blowing off the cold gases from the plasma nozzle shortly before the plasma was ignited. The range c in the measuring cycle relates to the plasma ignition process when the plasma power increases to the desired working power, during which the plasma’s jet thrust progressively increases. With constant power of the plasma torch the constant thrust of the plasma jet is achieved (range d). Turning the torch power off, the thrust abruptly falls to the starting value produced by a cold gas blow (range e) and further down to zero thrust when the gas flow is shut down (range f), which marks the end of the thrust measurement cycle. The recorded curve reveals good reproducibility of the conducted measurement. The estimated relative error of the calculated effective exhaust velocity (v_e) is $\pm 4\%$.

3. Results and discussion

All the results discussed here are obtained for argon/hydrogen plasma gas. The initial measurement of the U/I working regime showed that the PJ-100 gun possesses an ascending voltage–current characteristic in figure 5. The diameter of the cylindrical anode nozzle was 10 mm, and the total gas flow rate at 154 L min^{-1} was with 30% volume concentration of hydrogen.

Because of this working characteristic we decided to power the plasma gun by a power supply unit with a constant

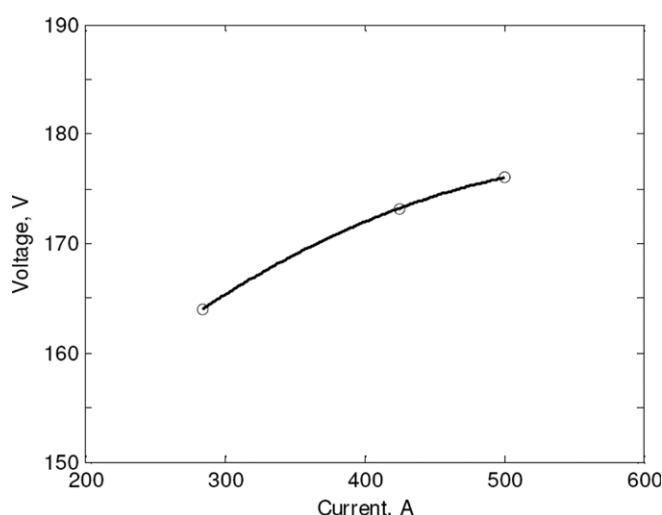


Figure 5. Voltage–current working characteristic of the PJ-100 gun.

voltage, instead of the conventional welding power supply unit, which has descending characteristics. Therefore, a transformer with discrete change for open-circuit voltages between 140 and 200 V was built, and the current control in the plasma generating gun circuit was achieved by a total plasma gas flow rate and by the concentration of hydrogen in the plasma gas mixture. High enthalpy two atomic gas hydrogen is used regularly in all existing plasma torches to control the plasma current and to increase the enthalpy of plasma. A ‘soft start’ of the PJ-100 is achieved by a ballast resistor, built into the current circuit, with continual regulation of resistivity from 150 m Ω at the moment of the plasma ignition down to zero, at the end of plasma ignition procedures. During this period, which lasts 5 s (range c in figure 4), the secondary plasma forming gas (hydrogen) is introduced to maintain the plasma current below a predetermined (fixed) value. This current maintenance process is controlled by a PLC unit (Programmable Logic Controller). Once the stable working regime is attained (without ballast resistivity) it is possible to achieve a fine tuning of the plasma current simply by manual control of the hydrogen flow rate. This current control principle is very sensitive to the percentage of hydrogen in the plasma forming gas mixture, which allows an easy and stable process of plasma generation

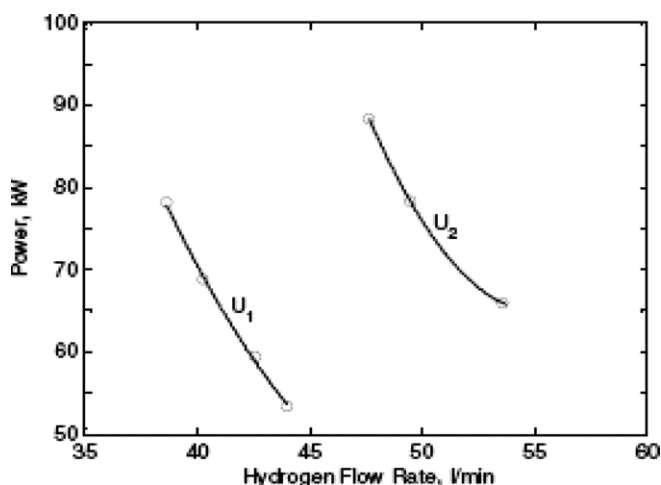


Figure 6. Plasma power versus the hydrogen flow rate; $U_1 = 164$ V and $U_2 = 174$ V.

Table 1. Basic working parameters of the PJ-100 plasma torch generating the argon/hydrogen plasma, at different open-circuit voltages.

U_0 (V)	P (kW)	η (%)	ω_{H_2} (L min ⁻¹)	H (MJ kg ⁻¹)	v_e (m s ⁻¹)	a_0 (m s ⁻¹)
190	70.0	73.7	53.8	15.5	593	2220
	80.0	73.9	49.5	17.6	733	2297
	90.0	72.7	47.7	19.3	880	2337
175	52.2	71.3	37.5	11.3	522	2041
	58.5	72.3	34.5	12.5	601	2136
	68.7	71.4	34.0	14.8	739	2209
	79.0	69.8	30.0	15.6	870	2258
158	43.4	71.7	26.5	9.3	484	1986
	48.5	73.6	25.0	10.6	546	2073
	58.8	71.6	21.5	12.8	673	2257
	68.4	70.2	17.0	13.8	799	2297

to occur using a gas valve with precise hydrogen gas flow rate regulation. This approach has proven to be a very good technical and engineering concept, which has considerably simplified the design of the power supply unit and offered a very stable power supply.

The change in plasma power with the change of the hydrogen flow rate is demonstrated in figure 6. At a constant flow rate of argon at 106 ± 0.5 L min⁻¹, it is possible to tune the working power of the plasma gun to any power between 60 and 90 kW (75 ± 15 kW), by changing the hydrogen concentration in the plasma gas mixture within a narrow interval, e.g. $\pm 2\%$ vol at 164 V and $\pm 2.5\%$ vol at 176 V.

This feature of the PJ-100 plasma installation can provide a wide range of enthalpies of the generated plasma. Table 1 shows the thermal efficiency coefficients for the gun, the plasma enthalpies generated by the 10 mm diameter anode nozzle and the 106 L min⁻¹ flow rate of the argon, values for effective exhaust plasma velocity (v_e) and estimated values for the sound velocity of the plasma jet. It can be seen from table 1 that a change in voltage from 158 to 190 V increased the power of generated plasma from 43.4 to 90.0 kW, increasing the enthalpy of the plasma plume from 9.3 to 19.3 MJ kg⁻¹.

The thermal efficiency of the plasma gun is between 70% and 74%. This rather high value is an excellent result for the new PJ-100 plasma torch and is astonishing, at first glance, because it would be expected that the thermal loss would increase with the increase in the arc length, because of an enlarged nozzle surface exposed to hot plasma.

Although the nozzle channel of the PJ-100 torch has a significantly larger water-cooled surface, the estimated thermal efficiency of this plasma torch is much higher than that of the conventional plasma torch and remains practically unchanged in a rather wide range of working powers tested.

Other authors have also acknowledged the effect of the thermal loss decrease with an ‘extended’ arc path of a bi-anodic plasma torch, where the anode nozzle of the conventional design was divided into two parts [12]. Such a torch could work in two modes: mode 1, when both anode segments were ‘earthed’, which is not unlike a conventional plasma torch, and mode 2, where only the segment further from the cathode tip was ‘earthed’, a design which resembles the PJ-100 torch.

All mechanisms of arc stabilization such as the wall stabilization, the vortex gas inlet and, to some extent, the effect of self-stabilization, due to the arc’s own magnetic field, jointly have an effect on the positioning of the core of the arc column alongside the axis of the anode channel.

The self-stabilization effect present in the pre-cathode part for arc currents higher than 50–100 A [13] ‘pushes’ the cathode jet in a direction normal to the cathode surface. The velocity of the cathode jet (v_{CJ}) can be estimated from the equation $v_{CJ} = I\sqrt{(\mu_0/2\rho)}/\pi b$ [14], where I (A) is the current, b (m) is the arc radius at the cathode, while ρ (kg m⁻³) is plasma density and $\mu_0 = 1.26 \times 10^{-6}$ N A⁻². In the case of our plasma generated with a current of 500 A, $b = 1.5 \times 10^{-3}$ m estimated to be an approximate radius of the ‘trace’, which the arc left on the cathode surface, we estimate the velocity of the cathode jet is higher than 200 m s⁻¹, which is many times higher than the gas velocity in the cathode section. Thus, the axially directed cathode jet is assisted by the effects of the vortex inlet of the cold gas and the walls of the anode channel, and these effects maintain the arc in the axis of the anode channel. This effect is very strong in the plasma column while it is in the zone of the inserted neutrode and substantially decreases any heat losses in this zone.

The largest heat loss occurs in the anode section where the arc root ends on the anode wall. In the anode section of the plasma torch the self-stabilization effect is substantially diminished as well as the vortex effect of the plasma gas. We consider that the significant heating of the gas achieved while it passes the lengthy anode channel contributes to a far more homogeneous radial temperature distribution in plasma and thence to a greater plasma speed. These effects probably influence to some extent the acceleration of plasma even in the cold boundary layer, enabling a far easier blowing of the arc root further downstream of the anode channel. Erosion scratches left by the arc root, figure 7(b), found alongside the anode wall, suggest this probable scenario.

As the length of the first 1/3rd of the anode channel, the narrow erosion scratches, of approximately 10–12 mm length, are visible in figure 7(b). The almost fully symmetric trace of

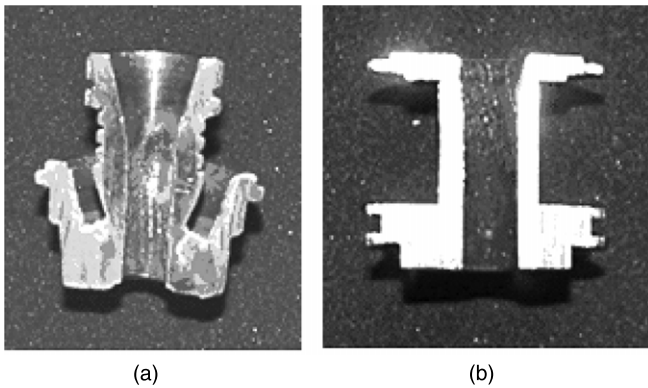


Figure 7. Photographs of the erosion paths at cut anodes: (a) Metco 7MB, 25–35 kW (courtesy of Inst. Nuclear Science, Vinca) and (b) PJ-100, 80–100 kW.

erosion in the inlet part of the anode is without any significant localized erosion. With an extended working time, the uniform erosion progresses, leading to a slightly conical shape of the anode in its inlet part as can be seen in figure 7(b) of an anode nozzle, which operated in the range 80–100 kW.

In the case of a conventional plasma torch the vortex gas inlet has as its function to rotate the anode spot more than to maintain the arc in the axis of the anode channel. Here due to the constructional feature of the torch's electrodes (the cathode protrudes into the anode space) the arc (current) path is nearly orthogonal to the axis of the anode channel. In this case, the self-stabilization effect in the cathode vicinity does not affect any thermal losses. The asymmetrically positioned arc in a conventional plasma torch is the main cause for any uneven plasma gas heating, which is conducive to high local heat transfer from the plasma to the anode. The direct consequence of this effect is that the plasma column in a conventional plasma torch has a considerably higher extent of convective heat transfer to the anode within a narrow zone of the anode channel in the vicinity of the cathode tip. Therefore, in the case of a conventional dc arc torch, the localized non-symmetrical erosion of the anode channel occurs within a distance of a couple of millimetres from the cathode tip [15]. This type of erosion is shown in figure 7(a) as a crater created at the cut of the conventional anode of the 7MB Metco plasma torch, which was working at a power three times lower than the PJ-100 torch. The traces of erosion visible in figure 7(b) were created during 80% of the total working time of 4.5 h at a power of 85 kW. The PJ-100 plasma torch worked in the power range 80–100 kW.

It is apparent from the data given in table 1 that the thrust of the plasma jet, i.e. the effective exhaust velocity of the plasma (v_e), increases with the working power of the plasma torch, i.e. with the plasma enthalpy. Based on the estimated values for v_e and a_0 it can be concluded that the effective exhaust velocity of the plasma jet is much lower than the sound velocity (25–30% of the sound velocity). These results lead to further optimization of the anode nozzle and two new anode nozzle designs; a cylindrical with $d = 8$ mm and a conical (7 mm/6°) nozzle.

3.1. Cylindrical versus conical anode nozzle

In this series of tests of the new nozzles, the plasma plume exiting the nozzle was photographed by the Imacon cameras simultaneously with thrust force measurements. The two photographs of the plasma plume, one exiting the cylindrical and the other the conical anode nozzle, working with a very similar power and gas flow rate are shown in figure 8.

It is apparent from the photographs in figure 8 that the textures and shapes of the plasma plumes for conical and cylindrical nozzles are very different. The plasma plume exiting the cylindrical nozzle is much longer, reaching a length of 60–70 mm. It can also be seen that the plasma plume generated in the conical anodic nozzle has a clear radial distribution of 'brightness'; it becomes less bright on the periphery. The plasma plume generated in the cylindrical nozzle has a far more uniform radial temperature distribution, observable by a far more uniform radial brightness of the plasma plume. None of the available light filters makes it possible to detect any change in brightness in the first half of the plasma plume length. This fact indicates that the first half of the plasma plume has a fully laminar flow.

The values of the basic working parameters of the PJ-100 plasma spraying torch, with two different nozzle designs, and the mean values of the plasma velocity (v) are estimated by measuring the photographed movement of the plasma 'clouds' as listed in table 2.

The mean values of the plasma jet velocity and standard deviations in table 2 show that the plasma jet generated in the cylindrical nozzle is faster and shows a smaller dissipation of estimated values than in the case of the conical anode nozzle. Greater dissipation of the mean plasma velocity for the conical anode nozzle is probably caused by a significant radial component of the plasma velocity, which is visible from the texture of the plasma plume in figure 8. The estimated values for the effective exhaust velocity of the plasma jet for conical and cylindrical nozzles show the same tendency as the plasma velocity obtained by photographing the movement of the plasma plume. Both measurement methods show that the plasma velocity exiting the conical anode nozzle is smaller than the plasma exiting the cylindrical nozzle. It was found that for both the cylindrical and conical anode nozzles the velocity obtained from a measured translation movement of plasma clouds is higher than the plasma velocity obtained by measuring the plasma thrust. The calculated effective exhaust velocities are higher for the plasma exiting the cylindrical nozzle ($d = 8$ mm) than for the conical nozzle (7 mm/6°). In the case of the tested conical anode nozzle the calculated effective exhaust velocity attained was 49% of the sound velocity, while in the case of the cylindrical nozzle, for the same power of 90 kW, the generated effective exhaust velocity of the plasma jet counts for 66% of the sound speed. In addition, the increase in power from 90 to 100 kW increased the mean thrust velocity to 70% of the sound velocity.

The values for plasma velocities obtained by the two adopted methods of measurements are rather close and the estimated differences are smaller in the case of the cylindrical nozzle. For instance, the velocity obtained by the photographing method in the case of the cylindrical nozzle

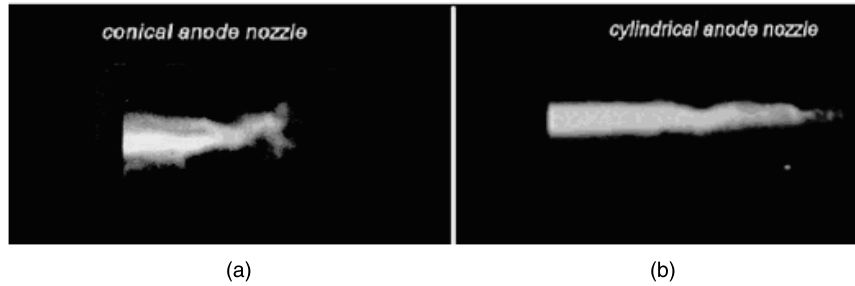


Figure 8. Shape and texture of the plasma plume exiting the conical and cylindrical anode nozzles ($P = 80\text{--}82\text{ kW}$).

Table 2. Working parameters of the PJ-100 torch and the achieved plasma jet velocity (v_e and v) for cylindrical and conical anode nozzles and $\omega_{Ar} = 94.7 \pm 0.9\text{ L min}^{-1}$.

Parameters	Conical nozzle 90 kW	Cylindrical 90 kW	Nozzle 100 kW
I (A)	480.0	498.0	546.0
P (kW)	90.000	91.134	99.370
ω_{H_2} (L min ⁻¹)	45.3	41.2	35.7
H (MJ kg ⁻¹)	23.2	23.3	24.1
v_e (m s ⁻¹)	1127 ± 45	1579 ± 63	1664 ± 67
v (m s ⁻¹)	1443 ± 356	1757 ± 226	
a_0 (m s ⁻¹)	2405	2396	2391

($d = 8\text{ mm}$) is 10% higher than the effective exhaust velocity, for the torch working power at 90 kW, and only 5% higher for power at 100 kW. The plasma velocity measured for the conical nozzle and torch power at 90 kW is 22% higher than the effective exhaust velocity. This significant discrepancy in the measured values was probably the result of greater thrust sensitivity on the radial velocity distribution across the plasma plume.

It might be expected that the plasma expands with a higher speed from a conical anode. Our measurements did not demonstrate this. This could be explained by the consideration of the heat energy transfer from the electric arc to the expanding gas in the anode channel. In order to achieve a higher expansion velocity from a conical anode channel, the completed process of heat transfer (from arc to gas) is required before the gas reaches the anode throttle. If attainable, such an ideal scenario would result in the attainment of definable P , T parameters of the plasma gas in the throttle of the anode channel. This condition is achieved only partially in the case of the conventional plasma gun due to the localized position of the arc in the vicinity of the cathode tip. In the case of the PJ-100 torch, the heat transfer to gas is stretched far from the anode inlet (throttle) compromising all the effects of expansion. Fluctuation of the arc root on the anode wall and transfer of heat from the arc to the gas cause local random fluctuations of pressure and temperature that are basic causes for the observed effect of any plasma turbulence. Therefore, in the case of the conical anode, we observed an increased effect of the radial turbulence during the gas expansion.

Although the widening angle of 6° is not excessive, it is possible that there is still a substantial suction of the surrounding air, which causes the cooling of the plasma jet which in turn can explain a lower speed of the plasma

expanding from the conical anode. Also, the plasma jet introduced into the anode nozzle is highly collimated after passing through a 32 mm long neutrode channel, contributing to a scenario where even the widening angle of 6° is still large enough to allow an efficient plasma jet expansion rather than air suction. Further measurements and testing are required for these two effects to be accurately assessed and possibly separated. It could be achieved either by construction of a conical anode with a cylindrical entrance extended to the anode zone where the erosion's scratches cease in the cylindrical anode or by testing anode nozzles with the widening angle further decreased.

4. Conclusions

The newly designed PJ-100 spraying plasma torch with its ascending voltage–current working characteristic was evaluated by measuring the basic working electro-thermal characteristics. An attained power of 100 kW with voltage in the order of 200 V and current up to 500 A enables the new plasma torch to work under a far more favourable current–voltage regime than the conventional plasma spraying torch, and yet achieve a considerably higher thermal efficiency of 70–74%.

A non-destructive method for plasma thrust measurement was adopted for the measurement of the plasma velocity. This direct measurement of the plasma thrust has proven to be very instrumental in the assessment of the plasma jet velocity in the development stages of the PJ-100 torch design. This method provided easy comparison of the thrust of the two plasma jets generated by different working parameters and by different anode designs.

The measured effective exhaust velocities (v_e) for the same working parameters of the plasma torch were compared with the plasma velocity obtained by measuring the downstream movement of the small plasma clouds of plasma plume (v), for both cylindrical and conical anode nozzles. The compared photographs of the plasma plumes exiting the cylindrical ($d = 8\text{ mm}$) and conical nozzles ($7\text{ mm}/6^\circ$) show that the plasma exiting the cylindrical nozzle has a more homogeneous radial temperature distribution, with a fully laminar flow in the first half of its length. Photographs of the plasma plume exiting the conical nozzle show a notable radial distribution of brightness, suggesting a significant radial distribution of the temperature and velocity.

The cylindrical nozzle generated a faster plasma ($v \approx 1800 \text{ m s}^{-1}$) when compared with the conical nozzle ($v \approx 1450 \text{ m s}^{-1}$). The same trend was obtained with a measured effective exhaust thrust velocity, giving $v_e \approx 1600 \text{ m s}^{-1}$ for the cylindrical and $v_e \approx 1100 \text{ m s}^{-1}$ for the conical nozzles. These velocities were always lower than the corresponding plasma velocities measured by the movement of the plasma clouds, most probably due to the greater sensitivity of the thrust measurement to the gradient of the radial velocity of the plasma plume.

Significant differences in dimensions, shapes and turbulence of the created plasma plumes and hence in the measured plasma velocities cause these two different plasma jets to have presumably very different coating capacities in the plasma spraying operation.

References

- [1] Schein J, Zierhut J, Dzulko M, Forster G and Landes K D 2007 *Contrib. Plasma Phys.* **47** 498
- [2] Fauchais P 2004 *J. Phys. D: Appl. Phys.* **37** R86
- [3] Barbezat G and Landes K 1999 *Sulzer Tech. Rev.* **4/99** 32
- [4] Bernecki F T *et al* 1988 Plasma gun with adjustable cathode *US Patent No* 4,780,591
- [5] Dorfman L P *et al* 1994 Vortex arc generator and method of controlling the length of the arc *US Patent No* 5,374,802
- [6] Tu X, Cheron B G, Yan J H and Cen K F 2007 *Plasma Sources Sci. Technol.* **16** 803
- [7] Vilotijevic M 2007 Dc plasma arc generator with increasing volt-ampere characteristic *RS Patent No* 49,706
- [8] Deininger W D, Pivrotto T J and Brophy J R 1990 *J. Propul.* **6** 271
- [9] Burton R L, Fleischer D, Goldstein S A and Tidman D A 1990 *J. Propul.* **6** 139
- [10] Rassel D A and Taborek P 1994 *J. Mater. Sci.* **29** 4683
- [11] Beason J *et al* 1996 Plasma spray nozzle with low overspray and collimated flow *US Patent* 5,573,628
- [12] Gao Y, An L, Sun C and Fu Y-Q 2005 *Plasma Chem. Plasma Process.* **25** 215
- [13] Boulos M I, Fauchais P and Pfender E 1994 *Thermal Plasmas: Fundamentals and Application* (New York: Plenum)
- [14] Reece Roth J 2001 *Industrial Plasma Engineering (Application to Nonthermal Plasma vol 2)* (London: CRC Press)
- [15] Li H-P and Chen X 2001 *J. Phys. D: Appl. Phys.* **34** L99–102